

Figure 4. Unit cell packing as viewed along the *b* axis.

UCl_3^+ cations,²⁵ and hydrated $\text{UO}_2(\text{NO}_3)_2$,²⁶ differs from those usually encountered with metal cations (e.g., K^+),²⁷ hydrogen-bonded molecules (e.g., malononitrile),²⁸ or cation-coordinated water (e.g., $\text{Mn}(\text{NO}_3)_2 \cdot 6\text{H}_2\text{O}$)²⁹ in that two *aga* units are replaced with *gga* units which allows two $\text{Sn}-\text{OH}_2$ groups to approach opposite sides of the ring to interact each with four ether oxygens (see stereoview in Figure 3).

Each of the two crystallographically independent tin atoms lying at a badly distorted O_h site [$\angle\text{C}-\text{Sn}-\text{C} = 154.4(2)^\circ$, $153.2(2)^\circ$] is coordinated to a water molecule *trans* to a $\mu\text{-Cl}$ atom of the central Sn_2Cl_2 ring. Such Cl-bridged Sn_2Cl_2 systems are found in $[\text{C}_6\text{H}_8]^+[(\text{CH}_3)_2\text{SnCl}_2]^-$ ($\angle\text{C}-\text{Sn}-\text{C} = 152.2^\circ$),³⁰ bis(dimethyltin dichloride-2,6-dimethylpyridine *N*-oxide) (145.3°),³¹ $[(\text{CH}_3)_2\text{SnCl}_2 \cdot \text{O}=\text{CC}_2(\text{C}_6\text{H}_5)_2]_2$ (142.2°),³² and $(\text{CH}_3)_2\text{SnCl}_2$ itself (123.5°).^{33,34} Of the five known examples, our $\mu\text{-Cl}-\text{Sn}$ distance is shortest.

Although crown ether complexes of tin(II) salts,^{35,36} triphenyltin(II) alkali-metal derivatives,³⁷ and inorganic^{38,39} and organotin(IV) halides and pseudohalides^{40,41} have been prepared, the only structural determination available shows O_h , *cis*-(H_2O)₂ SnCl_4 units hydrogen bonded to uncoordinated water and ether oxygen atoms in $\text{Sn}(\text{OH}_2)_2\text{Cl}_4 \cdot 18\text{-crown-6} \cdot 2\text{H}_2\text{O} \cdot \text{CHCl}_3$.⁴¹ Preparations of the title compound from methanol (mp 119–123 °C)⁴⁰ and isopropyl ether (mp 98–101 °C)⁴² give different melting points from our product (mp 132–138 °C) from chloroform, recrystallized from methylene chloride. From the tin-119m

Mössbauer [isomer shift = 1.59 ± 0.03 ; quadrupole splitting (QS) = $3.93 \pm 0.06 \text{ mm s}^{-1}$] QS value, an $\angle\text{C}-\text{Sn}-\text{C}$ angle of 160° can be calculated.⁴³

Acknowledgment. Our work is supported by the Office of Naval Research (to J.J.Z.). We thank M&T Chemicals, Inc., for the donation of organotin starting materials. Purchase of the University of Delaware X-ray diffractometer was supported by a grant from the National Science Foundation. We thank Dr. R. Harlow at the E. I. du Pont de Nemours and Co. for help with recording the low-temperature data set.

Supplementary Material Available: A listing of atomic coordinates and temperature factors (Table 1S), bond lengths (Table 2S), bond angles (Table 3S), anisotropic temperature factors (Table 4S), hydrogen coordinates (Table 5S), and observed and calculated structure factors (Table 7S) (18 pages). Ordering information is given on any current masthead page.

(43) Sham, T. K.; Bancroft, G. M. *Inorg. Chem.* **1975**, *14*, 2281.

Rate-Determining General-Base Catalysis in an Obligate le^- Oxidation of a Dihydropyridine

Ashoke Sinha and Thomas C. Bruice*

Department of Chemistry, University of California at Santa Barbara, Santa Barbara, California 93106

Received July 30, 1984

In the main, reduction reactions by dihydropyridines involve hydride transfer. Many proposals that the overall two-electron reductions of oxidants proceed by an initial electron transfer from dihydropyridine to oxidant have recently been shown to be faulted by the experimental methods employed to study these reactions.¹ There are, of course, examples of one-electron transfer from dihydropyridines.²⁻⁵ Experimental evidence has been offered in support of the following mechanism (eq 1) for the ferricyanide reaction.⁴ The rate-determining step, shown here in the ferricyanide oxidation of *N*-methylacridan (MH_2), is the general-base-catalyzed proton ionization (k_2).

- (1) Powell, M. F.; Bruice, T. C. *J. Am. Chem. Soc.* **1983**, *105*, 7139–7149.
Powell, M. F.; Bruice, T. C. *J. Am. Chem. Soc.* **1982**, *104*, 5834–5836.
(2) Schellenberg, K. A.; Hellerman, L. *J. Biol. Chem.* **1958**, *231*, 547.
(3) Carlson, B. W.; Miller, L. L. *J. Am. Chem. Soc.* **1983**, *105*, 7453–7454.
(4) Powell, M. F.; Wu, J. C.; Bruice, T. C. *J. Am. Chem. Soc.* **1984**, *106*, 3850.
(5) Okamoto, T.; Ohno, A.; Oka, S. *J. Chem. Soc., Chem. Commun.* **1977**, 181. Okamoto, T.; Ohno, A.; Oka, S. *Bull. Chem. Soc. Jpn.* **1980**, *53*, 330.

(25) Bombieri, G.; DePaoli, G.; Immirzi, A. *J. Inorg. Nucl. Chem.* **1978**, *40*, 1889.

(26) Bombieri, G.; DePaoli, G.; Immirzi, A. *J. Inorg. Nucl. Chem.* **1978**, *40*, 799.

(27) Dunitz, J. D.; Dobler, M.; Seiler, P.; Phizackerley, R. P. *Acta Crystallogr., Sect. B* **1974**, *B30*, 2733.

(28) Kaufmann, R.; Knöchel, A.; Kopf, J.; Oehler, J.; Rudolph, G. *Chem. Ber.* **1977**, *110*, 2249.

(29) Vance, T. B.; Holt, E. M.; Varie, D. L.; Holt, S. L. *Acta Crystallogr., Sect. B* **1980**, *B36*, 153.

(30) Buttenshaw, A. J.; Duchene, M.; Webster, M. *J. Chem. Soc., Dalton Trans.* **1975**, 2230.

(31) Ng, S.-W.; Barnes, C. L.; van der Helm, D.; Zuckerman, J. J. *Organometallics* **1983**, *2*, 600.

(32) Ng, S.-W.; Barnes, C. L.; Hossain, M. B.; van der Helm, D.; Zuckerman, J. J.; Kumar Das, V. G. *J. Am. Chem. Soc.* **1982**, *104*, 5359.

(33) Davies, A. G.; Milledge, H. J.; Puxley, D. C.; Smith, P. J. *J. Chem. Soc. A* **1970**, 2862.

(34) The two central, six-coordinated diphenyltin(IV) dichloride molecules in that tetrameric chain structure form a Cl-bridged Sn_2Cl_2 system (Bokii, N. G.; Struchkov, Yu. T.; Prokof'ev, A. K. *J. Struct. Chem. (Engl. Transl.)* **1972**, *13*, 619) with $\angle\text{C}-\text{Sn}-\text{C} = 125.5^\circ$ (Greene, T.; Bryan, R. F. *J. Chem. Soc. A* **1971**, 2549).

(35) Herber, R. H.; Smelkinson, A. E. *Inorg. Chem.* **1978**, *17*, 1023.

(36) Herber, R. H.; Carrasquillo, G. *Inorg. Chem.* **1981**, *20*, 3693.

(37) Bullard, W. R.; Taylor, M. J. *Aust. J. Chem.* **1981**, *34*, 1337.

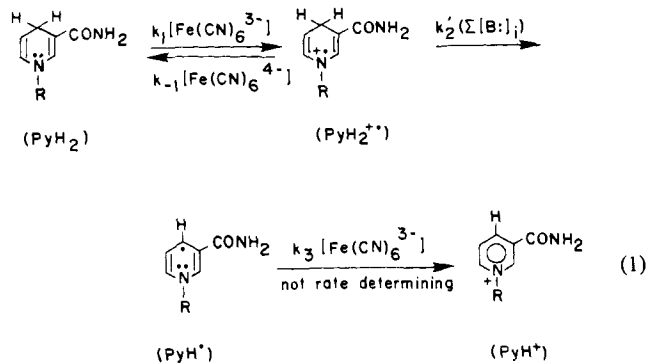
(38) Gur'yanova, E. N.; Ganyushin, L. A.; Romm, I. P.; Shcherbakova, E. S.; Movsumzade, M. J. *Gen. Chem. USSR (Engl. Transl.)* **1981**, *51*, 356.

(39) Cusack, P. A.; Patel, B. N.; Smith, P. J. *Inorg. Chim. Acta* **1983**, *76*, L21.

(40) Smith, P. J.; Patel, B. N. *J. Organomet. Chem.* **1983**, *243*, C73.

(41) Cusack, P. A.; Patel, B. N.; Smith, P. J.; Allen, D. W.; Nowell, I. W. *J. Chem. Soc., Dalton Trans.* **1984**, 1239.

(42) Russo, U.; Cassol, A.; Silvestri, A. *J. Organomet. Chem.* **1984**, *260*, 69.



The oxidation of MH_2 (4.7×10^{-6} M) has been studied under a nitrogen atmosphere in 20:80 acetonitrile–water (v/v) solvent at 30 ± 0.1 °C by following the increase in A_{355} with time under the pseudo-first-order conditions of $[\text{Fe}(\text{CN})_6^{3-}] \gg [\text{MH}_2] \ll [\text{Fe}(\text{CN})_6^{4-}]$ and at $[\text{K}^+] = 0.75$ M. From eq 1 there follows eq 2 by use of the steady-state assumption in MH_2^+ . In eq 2, k_{1y}

$$k_{\text{obsd}} = \frac{k_1[\text{Fe}(\text{CN})_6^{3-}](k_{1y} + k_2[\text{B}])}{k_{-1}[\text{Fe}(\text{CN})_6^{4-}] + k_{1y} + k_2[\text{B}]} \quad (2a)$$

$$\frac{1}{k_{\text{obsd}}} = \frac{K_{-1}[\text{Fe}(\text{CN})_6^{4-}]}{k_1[\text{Fe}(\text{CN})_6^{3-}](k_{1y} + k_2[\text{B}])} + \frac{1}{k_1[\text{Fe}(\text{CN})_6^{3-}]} \quad (2b)$$

represents catalysis by lyate species. It is evident from eq 2b that a plot of the reciprocal of the pseudo-first-order rate constant ($1/k_{\text{obsd}}$) vs. $[\text{Fe}(\text{CN})_6^{4-}]$ should yield as intercept $1/(k_1[\text{Fe}(\text{CN})_6^{3-}])$. In Figure 1 there is plotted $1/k_{\text{obsd}}$ vs. $[\text{Fe}(\text{CN})_6^{4-}]$ for experiments wherein $[\text{Fe}(\text{CN})_6^{3-}]$ was held constant (8×10^{-4} M). The values of $1/k_{\text{obsd}}$ fitted by line A were determined at pH 7.05 using 2×10^{-2} M imidazole/imidazolium ion as buffer. In the case of line B of Figure 1 the imidazole/imidazolium ion buffer was held at 2×10^{-1} M and pH varied from 6.40 to 7.69. The common intercept establishes that $1/k_1$ is not a function of the pH nor concentration of general-base species. Thus, any base catalysis of the overall oxidation must be accounted for in the conversion of MH_2^+ to MH . Employing constant concentrations of $\text{Fe}(\text{CN})_6^{3-}$ (8.0×10^{-4} M) and $\text{Fe}(\text{CN})_6^{4-}$ (1.5×10^{-4} M) the dependence of k_{obsd} upon buffer concentrations at varied constant pH values was determined for MH_2 and MD_2 . Buffers employed were imidazole/imidazolium cation, acetate/acetic acid, and formate/formic acid. Each buffer was studied at five pH values using five buffer concentrations at each pH. In the upper inset to Figure 1, the results of the buffer dilution experiments with imidazole buffer are displayed. The experimental data shown is representative, being in quality the same as obtained with both MH_2 and MD_2 and other buffers. The plots of the buffer dilution data follow the empirical rate given in eq 3 (where k'_{1y} represents

$$k_{\text{obsd}} = k'_{1y} + \frac{k'_B K_a [\text{B}]_t}{K_a + a_H} \quad (3)$$

apparent H_2O catalysis, k'_B the apparent second-order rate constant for buffer catalysis, and $[\text{B}]_t$ the total concentration of the buffer acid and buffer base). When $1/\text{slope}$ of the buffer dilution plots are plotted against activity of hydrogen ions (a_H), there is obtained as intercept $1/k'_B$ values and $1/k'_B K_a$ as secondary slopes. A plot of $1/\text{slope}$ vs. a_H for imidazole catalysis of the oxidation of MH_2 is shown in the lower inset of Figure 1. Similar plots were obtained when employing formate and acetate buffers.

The steady-state equation, eq 2a, for the mechanism of eq 1 and the observation of general-base catalysis dictates that $k_{-1}[\text{Fe}(\text{CN})_6^{4-}] \gg (k_{1y} + k_2[\text{B}])$. It follows, therefore, that the apparent second-order rate constant k'_B is related to the true buffer catalysis rate constant (k_2) by eq 4. From the known $[\text{Fe}(\text{CN})_6^{3-}]/[\text{Fe}(\text{CN})_6^{4-}]$ ratio (5.4) and the value of k_1 ($2.0 \text{ M}^{-1} \text{ s}^{-1}$) (determined from the intercept of Figure 1) the partition coefficient k_2/k_{-1} can be calculated. In a Brønsted plot of $\log(k_2/k_{-1})$ vs. pK_a of buffer acids for the oxidation of both MH_2 and MD_2 , the data points align along straight lines for both the MH_2 and MD_2 compounds with the points for H_2O catalysis exhibiting negative deviations of $\sim 10^2$. These features are as expected for a general-base-catalyzed reaction.⁶ The value of 0.2 for the slope of the Brønsted plots indicates that the transition state is early in the general-base-catalyzed proton-transfer reaction. Neglecting the secondary kinetic isotope effect on k_{-1} (donation of an electron by $\text{Fe}(\text{CN})_6^{4-}$ to MH_2^+ vs. MD_2^+) we can calculate the primary kinetic isotope effect $k_2^{\text{H,H}}/k_2^{\text{D,D}}$ to be 4.4 ± 0.1 for imidazole, acetate, and formate and 5.3 for water. The latter is identical with that obtained previously⁴ by a radiotracer technique. As in the case of the Brønsted β , the kinetic isotope effects indicate that in the rate-limiting step the transition state lies closer to the reactant species MH_2^+ than the product species MH . The values of the partition coefficients k_2/k_{-1} for MH_2 are 1.5×10^{-3} , 0.84×10^{-3} , 0.3×10^{-3} , and 3.9×10^{-7} for imidazole, acetate, formate, and H_2O , respectively. If one assumes the exergonic electron transfer from MH_2^+ to $\text{Fe}(\text{CN})_6^{4-}$ to be diffusion controlled ($10^{10} \text{ M}^{-1} \text{ s}^{-1}$) the values of the rate constants for proton transfer from MH_2^+ to general bases are $(1-5) \times 10^7 \text{ M}^{-1} \text{ s}^{-1}$ for imidazole, acetate, and formate and 10^4 for water. Both k_{-1} and k_2 represent second-order rate constants so that the partitioning of MH_2^+ is dependent upon $[\text{Fe}(\text{CN})_6^{4-}]$ and $[\text{buffer base}]$. Under the standard conditions of 1 M, $k_{-1}[\text{Fe}(\text{CN})_6^{4-}] \gg k_2$ [buffer base] and the general-base-catalyzed dissociation of the carbon acid MH_2^+ is rate controlling. The final piece of evidence required to substantiate the mechanism of eq 1 for an obligate le^- oxidation of a dihydropyridine has been put in place.

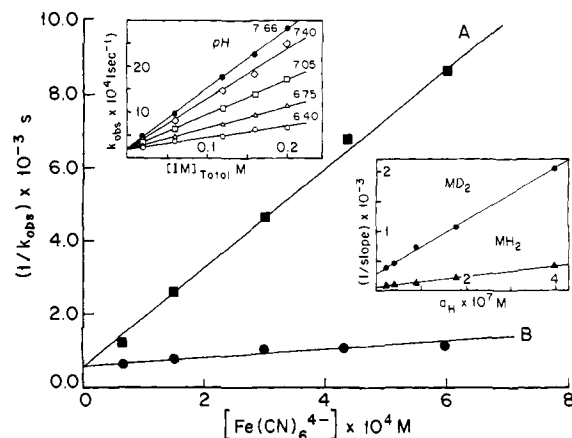


Figure 1. Plot of the reciprocal of the pseudo-first-order rate constant ($1/k_{\text{obsd}}$) vs. $[\text{Fe}(\text{CN})_6^{4-}]$ for the oxidation of *N*-methylacridan (MH_2) by $\text{Fe}(\text{CN})_6^{3-}$ (8×10^{-4} M) at pH 7.05 with total imidazole buffer $[\text{Im}]_t$ at 2×10^{-2} M (plot A) and at varying pH values (6.40–7.70) with $[\text{Im}]_t = 2 \times 10^{-1}$ M (plot B). Upper inset is a plot of k_{obsd} vs. $[\text{Im}]_t$ at the listed pH values. The lower inset is a plot of the reciprocal of the slopes (of plots of k_{obsd} vs. $[\text{Im}]_t$ for MH_2 and MD_2) vs. hydrogen ion activity.

$$k'_B = \left(\frac{k_1[\text{Fe}(\text{CN})_6^{3-}]}{k_{-1}[\text{Fe}(\text{CN})_6^{4-}]} \right) k_2 \quad (4)$$

$(\text{CN})_6^{3-}]/[\text{Fe}(\text{CN})_6^{4-}]$ ratio (5.4) and the value of k_1 ($2.0 \text{ M}^{-1} \text{ s}^{-1}$) (determined from the intercept of Figure 1) the partition coefficient k_2/k_{-1} can be calculated. In a Brønsted plot of $\log(k_2/k_{-1})$ vs. pK_a of buffer acids for the oxidation of both MH_2 and MD_2 , the data points align along straight lines for both the MH_2 and MD_2 compounds with the points for H_2O catalysis exhibiting negative deviations of $\sim 10^2$. These features are as expected for a general-base-catalyzed reaction.⁶ The value of 0.2 for the slope of the Brønsted plots indicates that the transition state is early in the general-base-catalyzed proton-transfer reaction. Neglecting the secondary kinetic isotope effect on k_{-1} (donation of an electron by $\text{Fe}(\text{CN})_6^{4-}$ to MH_2^+ vs. MD_2^+) we can calculate the primary kinetic isotope effect $k_2^{\text{H,H}}/k_2^{\text{D,D}}$ to be 4.4 ± 0.1 for imidazole, acetate, and formate and 5.3 for water. The latter is identical with that obtained previously⁴ by a radiotracer technique. As in the case of the Brønsted β , the kinetic isotope effects indicate that in the rate-limiting step the transition state lies closer to the reactant species MH_2^+ than the product species MH . The values of the partition coefficients k_2/k_{-1} for MH_2 are 1.5×10^{-3} , 0.84×10^{-3} , 0.3×10^{-3} , and 3.9×10^{-7} for imidazole, acetate, formate, and H_2O , respectively. If one assumes the exergonic electron transfer from MH_2^+ to $\text{Fe}(\text{CN})_6^{4-}$ to be diffusion controlled ($10^{10} \text{ M}^{-1} \text{ s}^{-1}$) the values of the rate constants for proton transfer from MH_2^+ to general bases are $(1-5) \times 10^7 \text{ M}^{-1} \text{ s}^{-1}$ for imidazole, acetate, and formate and 10^4 for water. Both k_{-1} and k_2 represent second-order rate constants so that the partitioning of MH_2^+ is dependent upon $[\text{Fe}(\text{CN})_6^{4-}]$ and $[\text{buffer base}]$. Under the standard conditions of 1 M, $k_{-1}[\text{Fe}(\text{CN})_6^{4-}] \gg k_2$ [buffer base] and the general-base-catalyzed dissociation of the carbon acid MH_2^+ is rate controlling. The final piece of evidence required to substantiate the mechanism of eq 1 for an obligate le^- oxidation of a dihydropyridine has been put in place.

Acknowledgment. This work was supported by a grant from the National Science Foundation.

Registry No. MH_2 , 4217-54-3; deuterium, 7782-39-0.

(6) Bell, R. P. "The Proton in Chemistry"; Cornell University Press: Ithaca, New York, 1973; p 200.